A Preliminary Study of Severe Wind-Producing MCSs in Environments of Limited Moisture

STEPHEN F. CORFIDI, SARAH J. CORFIDI, AND DAVID A. IMY

NOAA/NWS/NCEP/Storm Prediction Center, Norman, Oklahoma

ALLEN L. LOGAN

Lincoln University, Jefferson City, Missouri

(Manuscript received 2 September 2005, in final form 12 February 2006)

ABSTRACT

An examination of severe wind-producing mesoscale convective systems that occur in environments of very limited moisture is presented. Such systems, herein referred to as low-dewpoint derechos (LDDs), are difficult to forecast as they form in regions where the level of convective instability is well below that normally associated with severe convective weather. Using a dataset consisting of 12 LDDs that affected various parts of the continental United States, composite surface and upper-level analyses are constructed. These are used to identify factors that appear to be associated with LDD initiation and sustenance. It is shown that LDDs occur in mean kinematic and thermodynamic patterns notably different from those associated with most derechos. LDDs typically form along or just ahead of cold fronts, in the exit region of strong, upper-level jet streaks. Based on the juxtaposition of features in the composite analysis, it appears that linear forcing for ascent provided by the front, and/or ageostrophic circulations associated with the jet streak, induce the initial convective development where the lower levels are relatively dry, but lapse rates are steep. This convection subsequently grows upscale as storm downdrafts merge. The data further suggest that downstream cell propagation follows in the form of sequential, downwind-directed microbursts. Largely unidirectional wind profiles promote additional downwind-directed storm development and system sustenance until the LDD ultimately moves beyond the region supportive of forced convective initiation.

1. Introduction

High-wind- or derecho-producing mesoscale convective systems (MCSs) pose an important challenge to forecasters because of the widespread severe weather threats associated with them (Wakimoto 2001). In late spring and summer, derecho MCSs typically occur in environments of substantial convective instability, with very moist boundary layer inflow (Johns and Hirt 1987; Johns et al. 1990). During the cool season (October–March), when derechos are more commonly associated with amplifying disturbances in the westerlies, they occasionally occur in environments of only modest convective instability (e.g., Wolf 1998; Bentley and Mote 2000; Evans and Doswell 2001; Burke and Schultz 2004; van den Broeke et al. 2005). Nevertheless, lower-tropospheric moisture content in such situations typically is above seasonal norms.

More rarely, high-wind-producing MCSs occur in environments of very limited moisture, with surface dewpoints at or below 50°F (10°C) and/or precipitable water less than 0.5 in. (1.25 cm). Systems forming in such environments, herein referred to as low-dewpoint derechos (LDDs), have been observed throughout much of the year and over much of the United States from the Great Basin to the East Coast. Because they develop in environments of very low convective available potential energy (CAPE) not commonly associated with widespread severe convective weather (i.e., CAPE below 500 J kg^{-1}), LDDs are a challenge to forecasters (e.g., Fenelon 1998; Corfidi 2003).

This paper examines the synoptic- and meso-alpha-scale (Orlanski 1975) environment associated with 12 LDDs that have been identified over the continental United States since the mid-1970s. Emphasis is placed

Corresponding author address: Stephen F. Corfidi, NOAA/NWS/NCEP/Storm Prediction Center, 1313 Halley Circle, Norman, OK 73069.
E-mail: stephen.corfidi@noaa.gov

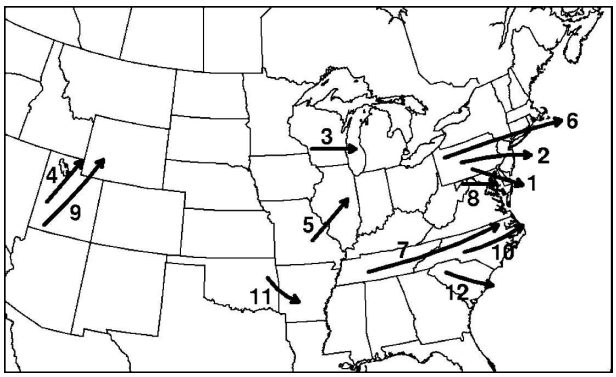

FIG. 1. Tracks of LDD centroids for the events studied. Numbers refer to the cases listed in Table 1.

on those factors that appear to be most strongly associated with LDD initiation, and how those factors promote system sustenance, in an attempt to better anticipate these uncommon events.

2. Data and methodology

The cases selected (Fig. 1 and Table 1) were chosen on the basis of data availability and knowledge of the events by the authors. The events included both warm and cool season LDDs that affected wide-ranging parts of the United States. These systems collectively caused scores of injuries and millions of dollars in property damage, as recorded in both the Storm Prediction Center (SPC) and *Storm Data* databases. Measured gusts in three cases exceeded 80 kt (40 m s^{-1}). Half of the events also produced hail, although most of this was marginally severe in size (diameter at or below 1 in. or 2.54 cm); several also produced brief tornadoes. All produced lightning, despite system cloud tops that averaged less than 30 000 ft (9 km) and in several cases were as low as 20 000 ft (6 km) AGL.

Surface and upper-air data were hand analyzed for each event to verify that the convective systems were surface based. Radar and satellite data were used (where available) to facilitate this process and to assist in the identification of thermal and moisture gradients. With one exception, each case had areal-averaged surface dewpoints at or below 50°F (10°C). This effectively excluded events involving strongly forced convective bands in environments of intense low-level shear and nearly moist-adiabatic thermodynamic profiles along wintertime cold fronts (e.g., van den Broeke et al. 2005); dewpoints in such situations typically are at or above 50°F (10°C). However, average surface dewpoints in one case (5 July 1997 in North Carolina) were near 62°F (17°C). This system was nevertheless included as moisture was unusually limited (precipitable water at or below 1.25 cm) and dewpoint depressions were unusually large [around 25°F (12°C)] for a day with widespread severe convection in that part of the country at that time of year. Radar data, ranging from manually digitized displays available from the National Climatic Data Center to single-site data from the Weather Surveillance Radar-1988 Doppler (WSR-88D) network, were examined to ascertain LDD initiation and motion. "Initiation" was defined as the time to the nearest half hour of the appearance of the first convective cells directly associated with the event. Visible and infrared satellite imagery provided valuable input for several of the more recent cases.

In accordance with Johns and Hirt (1987) and Coniglio et al. (2004), each LDD produced a continuous swath of nonrandom, convective wind damage and/or measured convective gusts in excess of severe limits [≥50 kt (26 m s^{-1})]. The pathlength criterion, however, was reduced from 400 to 200 km to allow for the inclusion of shorter-lived yet significant events (i.e., systems that would still require the issuance of watches and warnings). While this represents a significant deviation from the definition of derecho used in most previous studies, for the sake of simplicity, all of the systems in the present work will be referred to as LDDs. Because of known areal and temporal inconsistencies in the convective wind report database (Weiss et al. 2002; Doswell et al. 2005), a specific number of reports were not used as a minimum threshold criterion. That notwithstanding, it is worth noting that each case was associated with at least 10 separate reports of damaging wind and/or measured severe wind gusts; several produced more than 100 (Table 1).

Similar to the methodology followed by Johns et al. (1990), composite charts were prepared to depict mean observed conditions at the surface and at the 925-, 850-, 700-, 500-, and 250-mb levels.[1] While it would be advantageous to obtain composite data with greater vertical resolution, only the mandatory levels were sampled to keep the manual compositing process manageable. The data obtained for each event and for each level were collected using a 6 × 6 (36 point), 2400 km × 2400 km grid overlay. The resulting 450-km grid spacing roughly approximates that of the North American radiosonde network. This spacing was believed sufficient to resolve the salient features of the synoptic-scale LDD environment being investigated.

In contrast to Johns et al. (1990), the grid overlay was

[1] "Subterranean" data were omitted from the two cases that affected the Great Basin.

TABLE 1. Data for the LDD events studied. Sounding date and time refer to that of the radiosonde observation used in creation of the mandatory level composite maps. Initiation time is for the calendar date closest to the sounding date/time for the first storms directly associated with the LDD. Plus signs used under columns 7 and 9 (Duration and Length, respectively) denote cases for which severe weather was occurring as convective system moved beyond the continental United States. The letters C and W used in column 4 (LDD type) refer to cool and warm types, respectively (see text for details). Boldface in column 9 (Length) denotes systems that achieved derecho status as defined in previous studies (pathlength equal to or greater than 400 km). Boldface in column 10 (No. of reports) indicates occurrence of at least one significant [>65 kt (33 m s^{-1})] measured wind gust; italics in same column denote occurrence of at least one report of severe hail (diameter greater than or equal to 1.9 cm).

Case	Sounding date	Sounding time (UTC)	LDD type	Location (states affected)	Initiation time (UTC)	Duration (h)	Speed (m s^{-1})	Length (km)	No. of reports
1	9 May 1977	0000	C	PA and MD	2300	5+	14	250+	10
2	21 Nov 1989	0000	C	PA and NJ	2100	6+	21	**450+**	***150***
3	19 Apr 1994	0000	W	WI and MI	2230	4	21	300	14
4	31 May 1994	1200	C	UT and WY	1500	8	13	350	**16**
5	21 Nov 1994	0000	C	MO and IL	0400	4	25	350	**16**
6	4 Apr 1995	1200	C	PA and NY	1230	7+	26	**650+**	***100***
7	5 Jul 1997	0000	W	TN and NC	1830	10	25	**900**	*155*
8	14 Mar 2001	0000	C	VA and MD	0030	2	28	200	43
9	1 June 2002	1200	C	UT	1400	7	28	**700**	***44***
10	8 Mar 2004	0000	C	NC	2300	5+	20	350+	***22***
11	18 Mar 2004	0000	W	OK and AR	2300	4	28	300	18
12	5 Mar 2005	1200	C	SC	1700	3+	23	250+	14
Avg					2000	5+	23	420+	50

aligned along the direction of the predominant forward motion of the MCS, with the center of the grid placed on the centroid of damage and gust reports. This was done to account for the fact that LDDs, like all derechos, occur with a wide range of upper-jet orientations (e.g., from southwesterly to northwesterly; Coniglio et al. 2004). Because LDDs tend to move in the direction of the mean cloud-layer flow as do other fast-moving, forward-propagating convective systems (Corfidi 2003), this methodology resulted in the grids being oriented roughly parallel to the midtropospheric wind at the system centroids. Such orientation also minimized the loss of detail in the averaging process, which further serves to enhance the universal applicability of the results.

The composite data were analyzed by hand to ensure the maintenance of relevant thermal and moisture gradients. Average values of geopotential height, temperature, dewpoint, and wind speed and direction were calculated for every grid point at each level examined. Values were also tabulated for an additional point, the "centroid," located at the center of the grid. This location marked the midpoint of observed wind damage and/or severe gust reports for each event as contained in the SPC and *Storm Data* databases. A line drawn through the major axis of the reports was used to identify path direction, while the time and location of the first and last reports defined pathlength and duration. For the two cases that occurred over the Great Basin (31 May 1994 and 1 June 2002), it appeared that low population density may have negatively impacted the reporting of severe weather in parts of Utah and southwest Wyoming. As a result, radar and satellite data were used to extend the event pathlength and duration. Wind compositing in all cases was accomplished by calculating arithmetic means of direction and speed (Schaefer and Doswell 1979).

The radiosonde data times (0000 or 1200 UTC) selected for the creation of the upper-air analyses were believed to be most representative of the MCS initiation environment. The midpoint time of each event was less than 3 h from the selected radiosonde time for 8 of the 12 events. For four cases (31 May 1994, 21 November 1994, 1 June 2002, and 5 March 2005), the selected radiosonde time preceded the event midpoint by more than 3 but less than 6 h. The data, nevertheless, were still deemed representative of upper-level conditions at event initiation. Surface charts valid closer to the actual midpoint time of the LDD were used in these cases to better depict low-level conditions associated with MCS initiation.

The LDDs in this study exhibited comparatively short lifetimes (approximately 5 h) relative to the twice-daily radiosonde cycle and to the duration of most derechos (e.g., Coniglio et al. 2004). Because of this, no attempt was made to determine separate "beginning," "midpoint," or "end time" conditions as was done by Johns et al. (1990). Note, however, that five of the systems that affected the eastern United States were producing damaging winds as they moved into the Atlantic, and that two of the events persisted for more than 6 h.

3. Results

a. The synoptic environment

The composite charts given in Fig. 2 depict mean kinematic and thermodynamic patterns that differ notably from those normally associated with long-lived, warm season derechos (e.g., Johns et al. 1990). In particular, the flow is decidedly cyclonic at all levels in the LDD region. In this sense the synoptic environment most resembles the "upstream trough pattern" identified by Coniglio et al. (2004) in their observational study of derecho-producing convective systems. Environments of this type are characterized by the presence of a well-defined, progressive short-wave trough immediately upstream from the derecho location. Typically, such convective systems occur in close proximity to a maximum in the midtropospheric flow. The 500- and 250-mb composite charts (Figs. 2e and 2f) reveal that this is indeed true of LDDs, with the mean centroid located in the exit region of a mid- to upper-tropospheric jet streak.

While all of the LDDs studied occurred with cyclonic upper flow, the direction of orientation of the associated jet axis relative to the ground was quite variable. For example, the jet was oriented nearly meridionally (south-southwest to north-northeast) in the two cases that occurred over the Great Basin, while the background flow was west or northwesterly in the cases that affected the East Coast. The association of LDDs with west or northwesterly flow in the East may reflect the fact that low- to midlevel lapse rates (discussed in section 3b) tend to be greatest in that region during periods of persistent west to northwest flow. It is at these times that the lower-tropospheric environment is likely to be continental in origin. At the very least, the variability in jet orientations observed indicates that the kinematic and thermodynamic ingredients necessary for LDD genesis may be brought together by a wide range of large-scale upper-level flow regimes, much as is the case for derechos in general (e.g., Coniglio et al. 2004).

The surface, 925-mb, and 850-mb composites (Figs. 2a, 2b, and 2c, respectively) indicate that LDDs tend to occur within areas of enhanced low-level flow and thermal ridging ahead of strong cold fronts. These fronts appear to provide the necessary forced uplift that fostered initial convective development in each case examined. As might be expected given the amplified nature of the large-scale pattern, a well-defined couplet is apparent in the low-level thermal advection field. The convective systems occur near the center of the couplet, immediately downstream from a pronounced maximum of cold advection. The magnitude of the cold advection maximum is greater than that of the corresponding warm advection area located downstream from the LDD. This imbalance is also apparent at 700 and 500 mb (Figs. 2d and 2e, respectively), suggesting that the upstream short wave in an LDD environment typically is undergoing amplification via quasigeostrophic processes. Pronounced drying is also evident immediately upstream from the LDD location at both 700 and 500 mb.

The lower-tropospheric composite charts (Figs. 2a–c) reveal the recent passage of a trough or wind shift line in the vicinity of the system centroid. The trough may in part reflect the presence of the secondary or "southern stream" short-wave disturbance that is apparent at both 700 and 500 mb (Figs. 2d and 2e), with the low-level flow veering to a more system-parallel (generally westerly) direction in the wake of the trough. The feature appears to mark the onset of neutral or slight cold advection at low levels, and is therefore reminiscent of the prefrontal troughs described by Schultz (2005). In several individual cases, the trough appears to be thermal in origin, marking a maximum in the lower-tropospheric temperature field. The horizontal extent of the feature is much greater than that of most of the LDDs examined, suggesting that it is not simply a reflection of the convective systems themselves. The composite maps also indicate that the trough is associated with the leading edge of comparatively dry air advection at lower levels (Figs. 2a and 2b). The higher moisture values present downstream may, however, simply be an artifact of the data, as the cases included several eastward-moving systems over the mid-Atlantic region where a more maritime environment existed to the south and east.

b. Sounding and hodograph data

A mean sounding constructed from surface and mandatory level data for the LDD centroid location is shown in Fig. 3. The "smoothness" of the display reflects the limited vertical resolution of the data used in its creation as well as the averaging process. While the sounding must be interpreted with caution, major features of the LDD environment appear to have been preserved. In particular, the moisture profile depicts a lower-tropospheric environment that is quite dry relative to other organized severe convective weather situations; the mean relative humidity in the lowest 300 mb is 45%. As a result, there is considerable convective inhibition. The temperature profile, nevertheless, is one of notable conditional instability owing to the presence of lapse rates that are considerably greater than the climatological norm (Bluestein and Banacos 2002). This is especially apparent in the 850–500-mb layer,

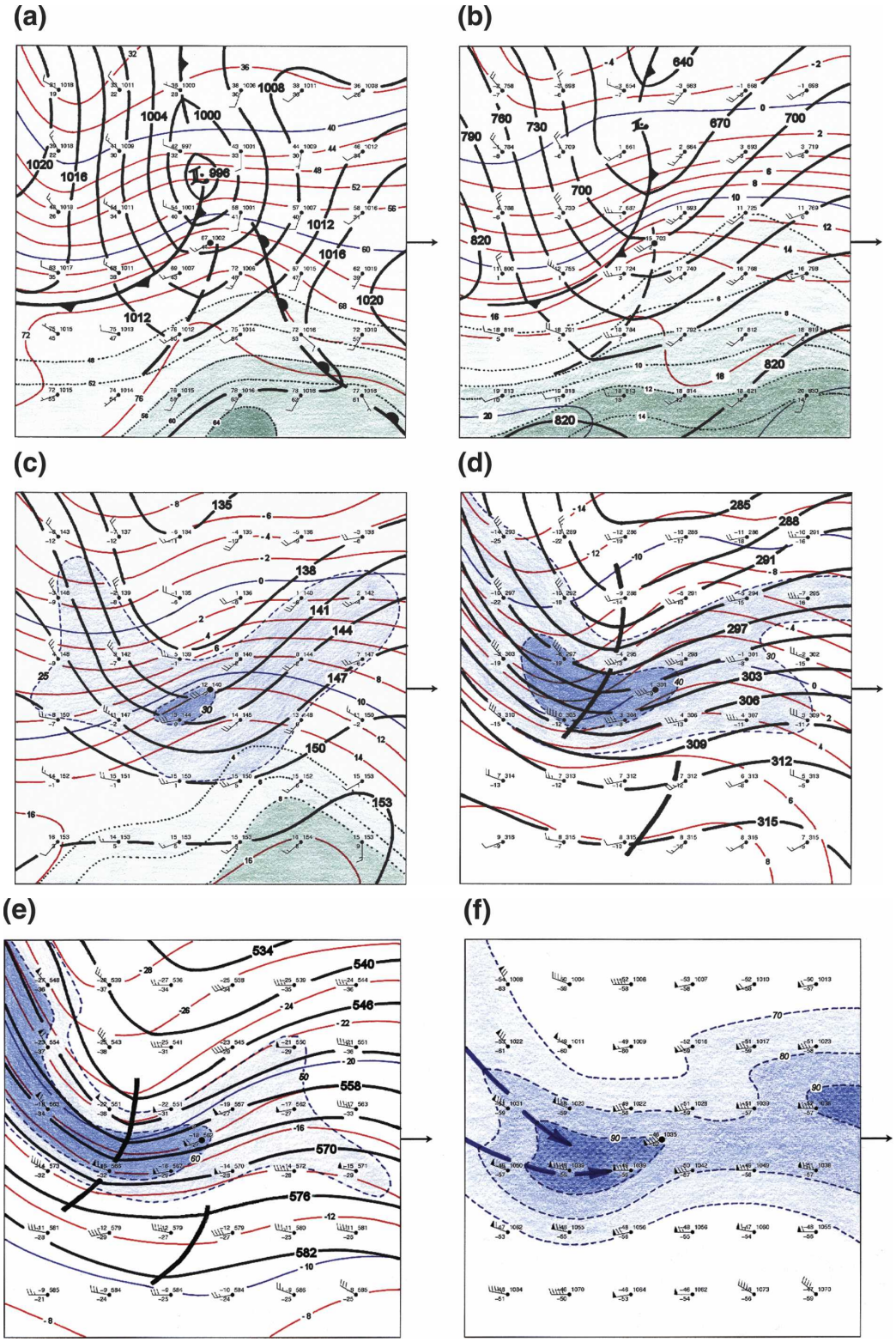

FIG. 2. Composite (a) surface, (b) 925-, (c) 850-, (d) 700-, (e) 500-, and (f) 250-mb analyses for the 12 LDD events studied: surface pressure (mb; thick lines) or geopotential height (dam; thick lines); and temperature [°C except °F in (a); solid red/blue thin lines] and dewpoint [°C except °F in (a); dotted green]. Temperature is contoured in 2° increments, except 4° in (a). Dewpoint is not contoured at 700, 500, and 250 mb; temperature and height are not contoured at 250 mb. Wind speed is in knots [half barb = 5 kt (2.5 m s^{-1}), full barb = 10 kt (5 m s^{-1}), and pennant = 50 kt (25 m s^{-1})]. Isotachs (kt) are shown at 850, 700, 500, and 250 mb (dashed blue). Jet axes at 250 mb are depicted by dark blue arrows in (f). Enlarged station circles (black dots) in the center of each figure represent LDD centroid; arrows on the right side indicate time-averaged direction of LDD motion.

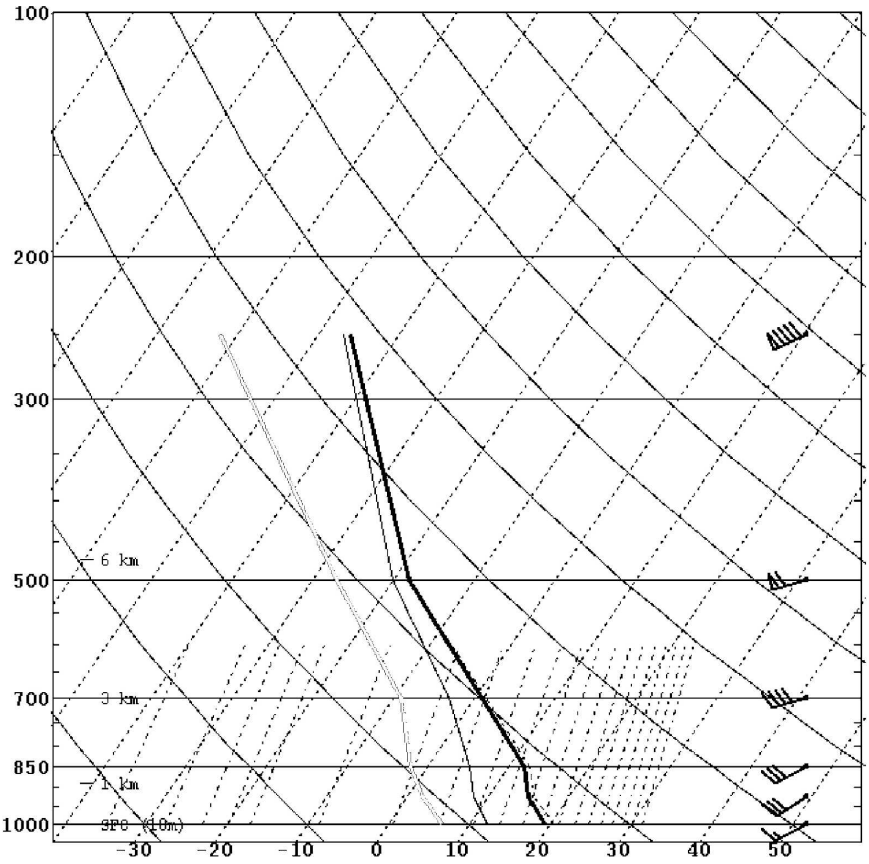

FIG. 3. Mean sounding for LDD centroid location: temperature (thick black); dewpoint (gray); and wet-bulb temperature (thin black). Surface data plotted at 1000 mb. Wind speed is in knots [half barb = 5 kt (2.5 m s^{-1}), full barb = 10 kt (5 m s^{-1}), and pennant = 50 kt (25 m s^{-1})]. Wind directions are relative to system motion (see also Fig. 5).

where the mean lapse rate exceeds 7.0°C km^{-1}. Assuming that moist convection is able to breach the weak inversion present at 850 mb, the combination of steep low- to midlevel lapse rates and large temperature–dewpoint spreads suggests a mean thermodynamic environment that is amply suited for strong convective downdraft development (Wakimoto 1985).

To further investigate the thermodynamic environment of LDDs, plan-view plots of mean low- to midlevel lapse rates are provided in Fig. 4. These charts indicate that while the low-level LDD environment is indeed unsaturated, there exists a considerable degree of conditional instability. For example, in the 850–700-mb layer (Fig. 4a), lapse rates reach a maximum of 7.2°C km^{-1} at the LDD centroid. A rather sharp gradient in the lapse rate field is also apparent to the left of the direction of LDD motion (facing downstream), with steeper lapse rates to the right (i.e., in the general direction of the 850- and 700-mb inflows; see Figs. 2c and 2d), and substantially more stable conditions to the left. The lower-tropospheric instability is surmounted by instability in the 700–500-mb layer (Fig. 4b), although the horizontal lapse rate gradients in this layer are diminished. A lapse rate maximum is also apparent in the vicinity of the system centroid through the depth of the entire lower troposphere (Fig. 4c). By comparison, however, the degree of instability in this deeper layer is rather weak, owing to the weaker lapse rates present below 850 mb (see Fig. 3).

The steep lapse rates associated with LDDs are noteworthy considering that 1) most of the cases examined occurred in areas far removed from the strongly mixed boundary layer environments of the western United States (typical source region of elevated mixed layers over the central and eastern states) and that 2) half of the events took place during the cool season (October–March). The degree of conditional instability associated with the 850–700-mb layer is also notable considering that the climatological areal-averaged lapse rates in that part of the troposphere range from near moist adiabatic to isothermal over the central and eastern United States (Bluestein and Banacos 2002).

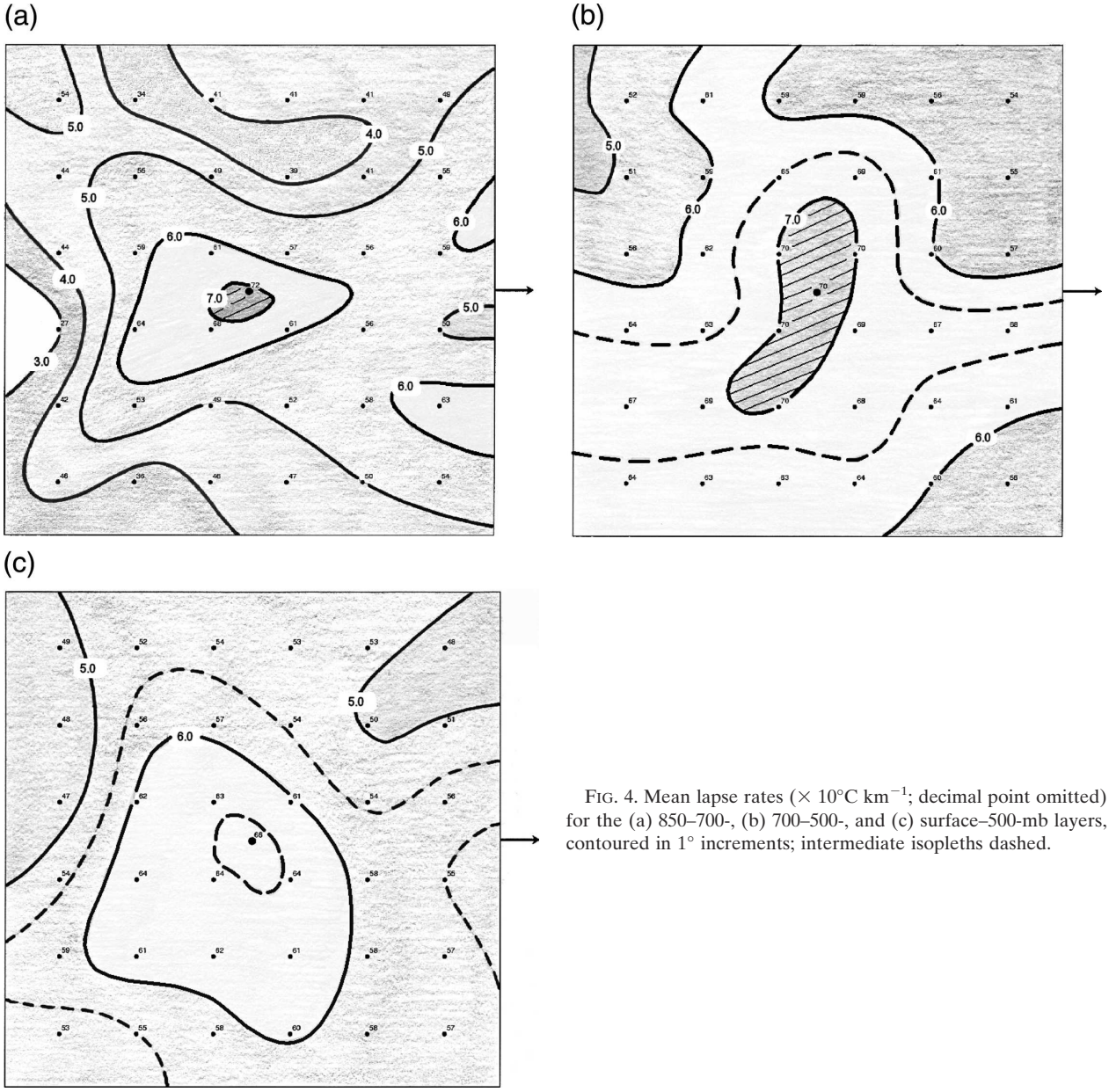

FIG. 4. Mean lapse rates ($\times$ 10°C km^{-1}; decimal point omitted) for the (a) 850–700-, (b) 700–500-, and (c) surface–500-mb layers, contoured in 1° increments; intermediate isopleths dashed.

Figure 5 is a mean hodograph constructed from surface and mandatory level data for the LDD centroid. Recall from the compositing procedure that wind directions are relative to system movement, with the *x* axis oriented parallel to the observed system motion (denoted by the black dot). It is apparent that the systems move slightly to the right of the wind at all levels. This reflects the contribution of propagation (i.e., the development of new convective cells relative to existing activity) to total system motion, and is consistent with Fig. 4, which shows that the greatest low-level instability is typically located to the right of LDD motion. The hodograph is rather linear, exhibiting moderate to strong shear that increases monotonically through 250 mb (end of hodograph). While shear in the lowest 1 km is quite modest [14 kt (7 m s^{-1})], the mean surface–6-km shear is nearly 75 kt (38 m s^{-1}). The strength of the deep shear reflects the baroclinic nature of the environments in which LDDs occur. By comparison, Coniglio et al. (2004) found the mean 0–1- and 0–6-km shear to be 30 kt (15 m s^{-1}) and 54 kt (27 m s^{-1}), respectively, for strongly forced derechos. That a greater degree of shear is distributed aloft in LDD environments perhaps reflects that the boundary layer is more deeply mixed

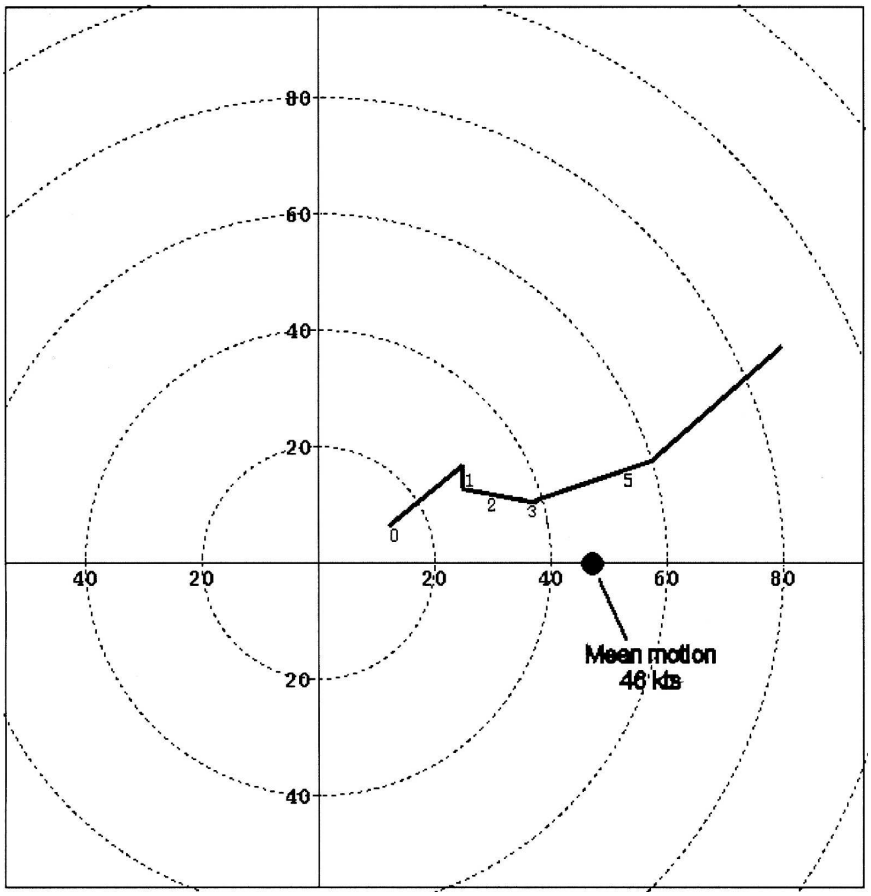

FIG. 5. Mean hodograph for LDD centroid location, with speed rings labeled in knots. Numbers along hodograph give height in kilometers AGL. The *x* axis is oriented parallel to the direction of observed mean LDD motion, with the speed of mean motion [46 kt (23 m s^{-1})] given by the black dot.

with LDDs than is the case with other strongly forced derechos.

c. Discussion

The black dot in Fig. 5 depicts the speed of the average forward motion of the LDDs studied: 46 kt (23 m s^{-1}). This is faster than the mean environmental flow [43 kt; (22 m s^{-1})] and represents unusually deep (about 4 km) front-to-rear inflow, considering that the average tops of the convective systems were approximately 9 km. The presence of deep front-to-rear flow (relative to cloud depth) sets LDDs apart from other strongly forced derecho-producing systems, which have, by comparison, shallower system-relative inflow (Evans and Doswell 2001; Coniglio et al. 2004). *Deep front-to-rear flow, thermodynamic environments that are favorable for the development of strong, low-level convective downdrafts, and the fact that LDDs move faster than the mean wind all suggest that propagation likely plays a disproportionate role in LDD movement* (relative to advection) compared with other strongly forced MCSs.[2]

The notion that propagation plays a particularly important role in LDD motion is supported by the examination of radar reflectivity data from several of the LDDs in this study. Individual storms within the LDDs typically are weak (radar reflectivities less than 40 dB*Z*) and often persist for less than 1 h. But the convective systems as a whole appear to be maintained by the sequential development of new cells that form in the downstream direction (forward propagation) along gust fronts produced by existing storms. This process is

[2] Recall (e.g., Chappell 1986 and references therein) that total MCS motion may be decomposed into two parts: 1) an advective component associated with the movement of embedded convective cells by the mean wind and 2) a propagation component reflecting the development of new cells relative to existing storms.

most readily apparent in animated radar imagery (two reflectivity loops and a visible satellite loop are available as supplemental material at the Journals Online Web site: http://dx.doi.org/10.1175/WAF947.s2, http://dx.doi.org/10.1175/WAF947.s3, and http://dx.doi.org/10.1175/WAF947.s4), although it is sometimes also evident in sequences of still images such as those in Fig. 6. The images in Fig. 6 depict part of the evolution of an LDD that moved across coastal South Carolina (case 12 in Table 1). Especially in the region just east of Charleston, individual convective elements may be tracked as they consecutively are "undercut" by the system's east-southeast-moving outflow boundary (downwind from black arrows in Figs. 6a–c). The boundary, in turn, then serves to initiate a new band of storms as it moves off the South Carolina coast after 2205 UTC (Figs. 6d–f).

Occasionally, the role of forward propagation in LDD motion is also apparent in geostationary satellite imagery. The visible data sequence in Fig. 7 shows old convective cells being "left behind" atop post-LDD outflow as new storms form on the northeast-moving gust front associated with the 31 May 1994 Utah LDD (case 4 in Table 1; a visible satellite loop is available as supplemental material at the Journals Online Web site: http://dx.doi.org/10.1175/WAF947.s1). While the degree of forward propagation apparent in this example is particularly striking, it is recognized that forward propagation occurs to some extent in many types of MCSs, and that not all systems exhibiting rapid forward propagation are LDDs. Instead, the low ambient relative humidity of the LDD environment tends to minimize the coverage of auxiliary clouds. As a result, it may be that cell propagation is simply more readily observable in LDDs than is the case with systems that occur in more humid regimes.

Another characteristic of the LDD environment that fosters forward propagation is apparent in the wind profile shown in Fig. 3. The profile is not only strong, but also nearly unidirectional. Strong, unidirectional wind fields are known to favor coherent motion of storm-scale downdrafts and to promote rapid elongation of the resulting MCS cold pool in the downstream direction (Corfidi 2003). This can strengthen and deepen low-level system-relative inflow and therefore promote convective initiation and sustenance in relatively dry conditions by forcing parcels to the level of free convection.

Considering the overall kinematic and thermodynamic environment that has been presented, a picture of LDD development and sustenance begins to emerge. First, forced ascent promotes convective initiation along a sharp cold front or prefrontal wind shift line. Forward propagation of this activity is then fostered by a combination of linear forcing (provided by the front) and the presence of moderate to strong unidirectional flow. Coupled with the presence of a thermodynamic environment that is conducive to the formation of strong convective downdrafts, the setup is one that appears to support an "organized microburst" convective mode. Successive microburst production allows for discrete downstream propagation of the nascent convective system. In short, the evidence suggests that *LDDs may be bands of downwind-directed microbursts.* With new cell development focused in the same direction as the mean flow, the advective and propagational components of system motion are additive. As a result, depending upon the rate of downstream development, LDD movement may considerably exceed that of the mean wind. It is further conjectured that the LDD regeneration process via forward propagation continues until the system ultimately moves into a region that is no longer supportive of forced convective initiation and subsequent cold downdraft production.

As might be expected given the rapid motion of the organized downdrafts, radar data show that the cells composing LDDs frequently assume a bow configuration (e.g., Przybylinski 1995). This configuration can occur on various length scales ranging from that of individual cells to bands of storms extending 100 km or more (e.g., Fig. 6). In several of the events examined, bowing appeared to follow periods of especially rapid downstream propagation and/or episodes of locally enhanced downward momentum transfer. Bow structures are certainly characteristic of LDDs. It should be emphasized, however, that LDDs are probably most noteworthy for the relatively weak reflectivities (usually less than 40 dBZ; sometimes less than 20 dBZ) displayed through the duration of the event. Another radar aspect is the absence of long-lived, embedded storms. Considering what has been said regarding the role of discrete propagation and sparse moisture in contributing to LDD behavior, these two observations are not surprising. The radar presentations of two recent LDDs will be discussed briefly in the next section.

4. "Cool" and "warm" LDDs

a. Comparison data

A review of the individual upper-air and sounding analyses used in this study reveals that while the LDD environments are similar in many respects, two broad classes of events may be distinguished. The first of these most closely resembles the mean pattern described in the previous section, with decidedly cyclonic flow

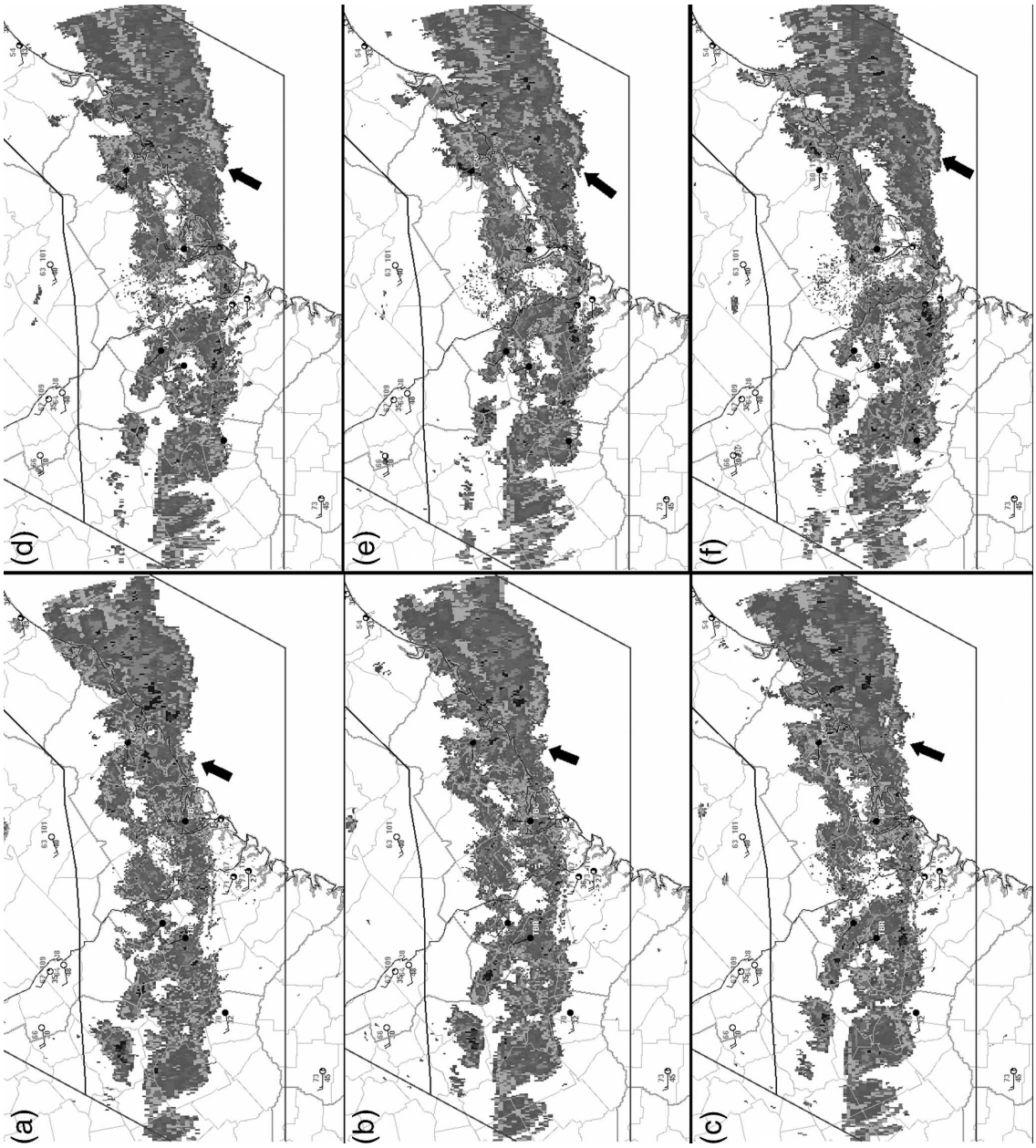

FIG. 6. Sequence of WSR-88D 0.5° base reflectivity data from Charleston, SC, at (a) 2140, (b) 2148, (c) 2157, (d) 2205, (e) 2214, and (f) 2222 UTC 5 Mar 2005. Surface data depicted in standard station model format: temperature and dewpoint (°F), pressure (tenths of a mb) with leading 10 omitted, wind speed [half barb = 5 kt (2.5 m s^{-1}), full barb = 10 kt (5 m s^{-1})], and sky condition. Black lines delineate a severe thunderstorm watch issued by NOAA/SPC for this event. See text for discussion of areas highlighted by black arrows.

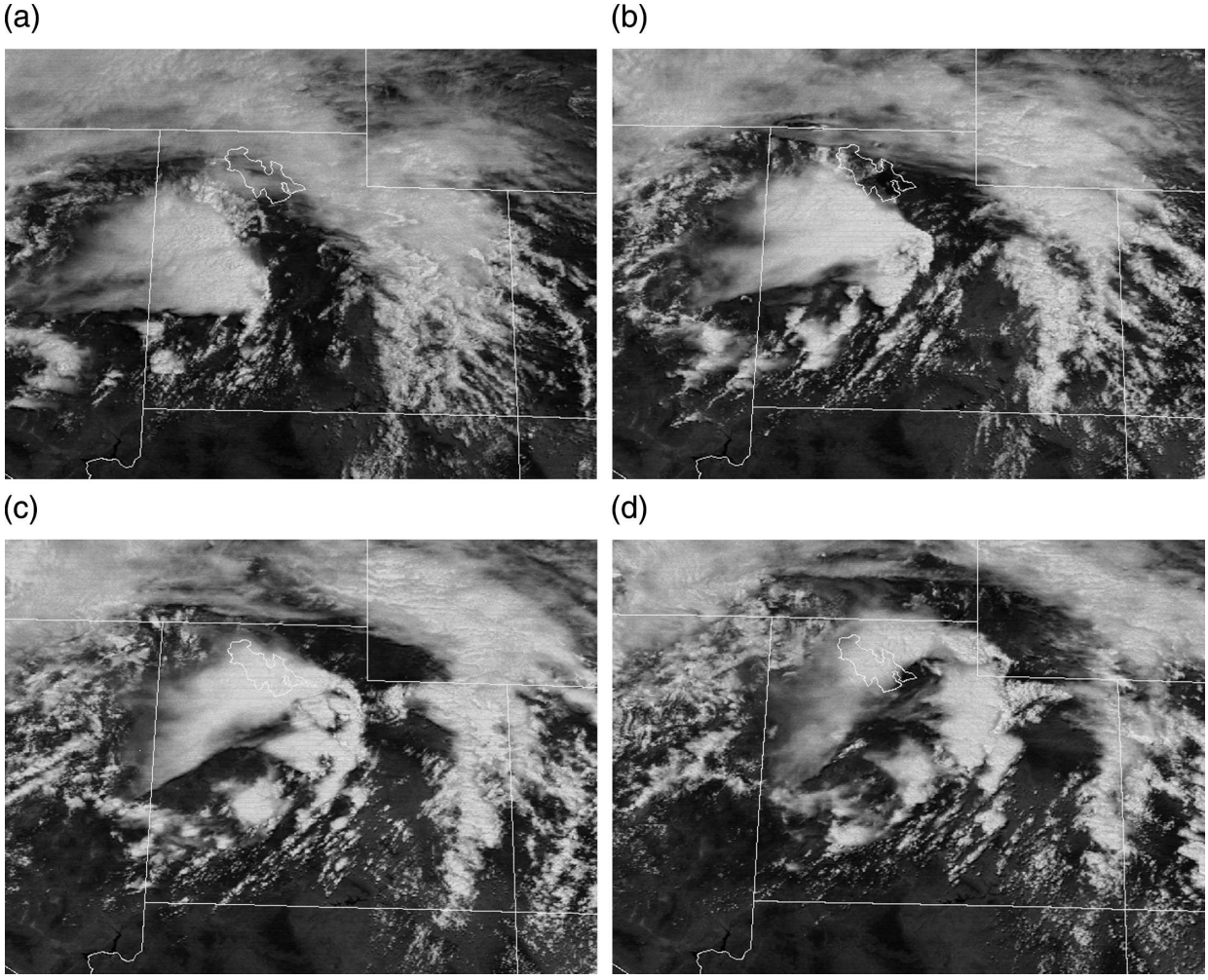

FIG. 7. Sequence of Geostationary Operational Environmental Satellite visible data satellite imagery showing northeastward motion of an LDD over western and northern UT at (a) 1800, (b) 1900, (c) 2000, and (d) 2100 UTC 31 May 1994.

present at all levels. Nine of the 12 cases examined were of this type, which, for the purpose of discussion, will be referred to as cool events. The second pattern, represented by the remaining three cases, is characterized by somewhat weaker and less cyclonic upper-level flow. More significantly, systems of the latter type occur in comparatively warm tropospheric regimes with very deep convective boundary layers. These LDDs herein will be referred to as warm events. Table 1 provides a listing of the cool and warm cases identified.

Differences in the two classes of events are evident in the comparison soundings and hodographs given in Figs. 8 and 9, respectively. While the limited sample size and compositing process once again dictate that the data be interpreted with caution, notable differences between the two subgroups are apparent. For example, the cool LDD environment exhibits a weak inversion between 925 and 850 mb, while the warm temperature profile depicts a mixed layer that extends to at least 700 mb. Because four of the cool event soundings were taken at 1200 UTC, the inversion could reflect, in part, the influence of nocturnal cooling. The warm composite exhibits a moisture discontinuity at 925 mb. Such a feature does not support the deeply mixed environment suggested by the temperature profile, and may be an artifact of the small sample size and/or the use of mandatory level data. Observed warm event proximity soundings (e.g., Fig. 11b) show only slight departures from a deeply mixed dewpoint profile. Interestingly, however, weak low-level moisture discontinuities are also apparent in the evening soundings presented by Wakimoto (1985; his Fig. 6) for dry microburst days in warm, deeply mixed boundary layers over the High Plains.

The comparison hodographs (Fig. 9) reveal that warm LDDs move closer to the direction of the mean

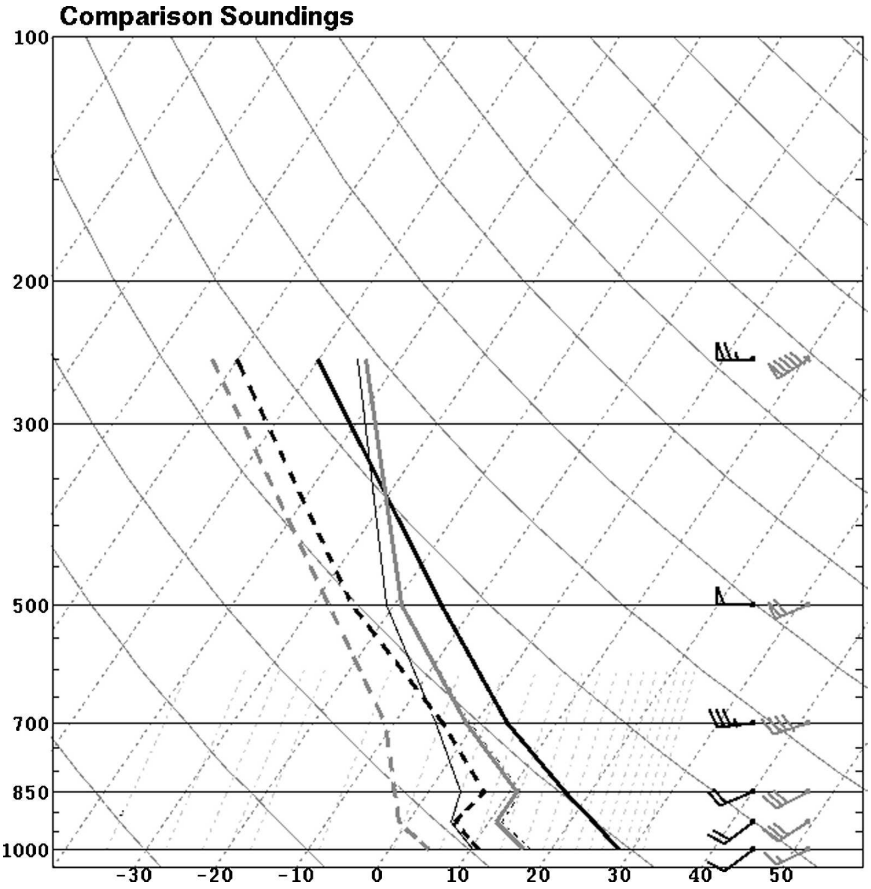

FIG. 8. Comparison of mean soundings for the nine cold events: temperature (solid gray); dewpoint (dashed gray); wind barbs (gray); and wet-bulb temperature (thin black) and three warm events: temperature (thick black); dewpoint (dashed black); and wind barbs (black). Wind data are as shown in Fig. 3.

flow than do cool systems (the warm hodograph lies close to the *x* axis). This suggests that warm events tend to occur in the presence of more expansive surface-based instability relative to the strongly cyclonic cases, resulting in less propagation to the right of the mean flow. Indeed, the warm sector was comparatively broad in the vicinity of the three warm systems relative to most of the cool events. The small size of the data subset, however, precludes a definitive statement. The hodographs also imply that warm LDDs experience deeper front-to-rear flow than do cool events. This is apparent from the fact that the warm systems move faster than the environmental flow at all levels except the highest, whereas the cool LDDs move with the speed of the flow in the 3.5–4.0-km layer. The more rapid relative motion of the warm systems implies that propagation accounts for a greater part of system motion than is the case for cool events. This is consistent with Evans and Doswell (2001) who suggested that propagation plays an increasingly significant role in MCS motion the weaker the large-scale forcing. Coupled with the modest degree of low-level veering and implied warm advection indicated in the hodograph, warm LDDs may be regarded as drier versions of the "progressive" derechos described by Johns (1993).

b. Example cases

An example of a cool or strongly cyclonic LDD that affected parts of North Carolina and southern Virginia on the evening of 7 March 2004 (case 10 in Table 1) is given in Fig. 10. The convective system preceded an intense Ohio Valley disturbance (Fig. 10a) that was accompanied by 500-mb wind speeds in excess of 120 kt (60 m s^{-1}). Surface dewpoints ahead of the associated cold front in central North Carolina were between 0° and 5°C. Coupled with afternoon dry-bulb readings near 20°C, this yielded dewpoint depressions of 15°–20°C (Fig. 10b).

The radar sequence in Fig. 10c illustrates the com-

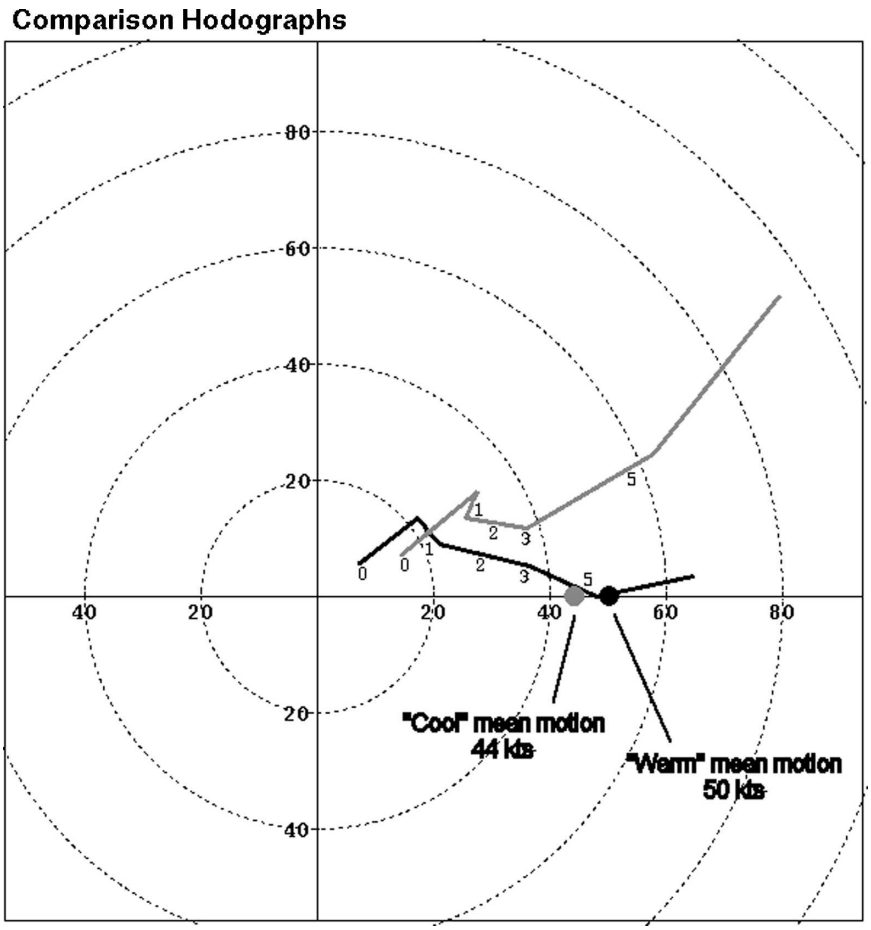

FIG. 9. As in Fig. 5 but for the nine cold (gray line) and three warm (black line) events. Numbers on hodographs give the height in kilometers. The mean motion for cool and warm events is depicted by gray and black dots, respectively.

paratively weak and short-lived cells that are characteristic of cool LDDs (a base reflectivity loop is available as supplemental material at the Journals Online Web site: http://dx.doi.org/10.1175/WAF947.s5). Maximum echo strengths of the wind-producing cores remained at or below 40 dBZ. The evolution of this particular event was complicated by the fact that the original gust front and its associated downward momentum surge evolved from post–cold frontal (elevated) convection that formed over western North Carolina and southern West Virginia (not shown). This activity later merged with prefrontal storms that formed over the North Carolina Piedmont. The latter storms appear as the isolated, orange-colored (40–45 dBZ) cores northwest of the radar site at 0031 UTC in Fig. 10c. The LDD continued to produce isolated damaging wind gusts until it moved off the North Carolina and Virginia coast at 0500 UTC.

Figure 11 depicts a warm event that moved southeast across western Arkansas on the evening of 18 March 2004 (case 11 in Table 1). This LDD evolved from a cluster of storms that developed during the late afternoon over eastern Oklahoma ahead of a weak midlevel trough (Fig. 11a). Substantial surface heating that occurred prior to MCS development yielded a deeply mixed boundary layer, with temperature–dewpoint spreads of up to 20°C in western Arkansas (Fig. 11b). This promoted the development of strong convective downdrafts and new cell formation on the merging gust fronts produced by the initial storms. The largely unidirectional west-northwesterly cloud layer flow, in turn, hastened downstream propagation and consolidation of the activity into a forward-propagating system (Fig. 11c; a base reflectivity loop is available as supplemental material at the Journals Online Web site: http://dx.doi.org/10.1175/WAF947.s6). In contrast to the other two warm events examined, the distribution of surface-based instability ahead of the incipient LDD was nonuniform; CAPE was greatest over eastern Oklahoma and decreased eastward into Arkansas where both tempera-

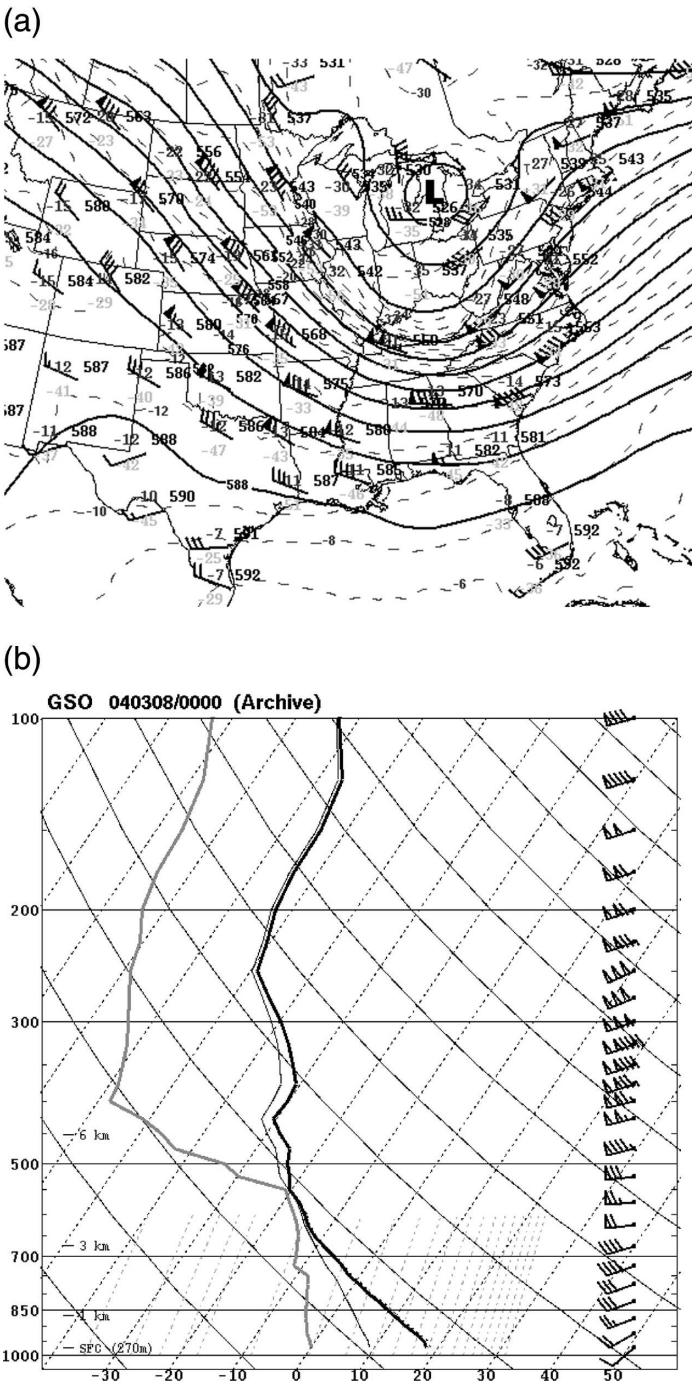

FIG. 10. (a) The 500-mb analysis at 0000 UTC 8 Mar 2004. Standard station model format used: temperature and dewpoint (°C), height (dam), and wind [half barb = 5 kt (2.5 m s^{-1}); full barb = 10 kt (5 m s^{-1}); and pennant = 50 kt (25 m s^{-1})]. Height contours (solid black; 60-m intervals) and temperature contours (dashed gray; 2° intervals) are shown. (b) Radiosonde observation at Greensboro, NC, at 0000 UTC 8 Mar 2004. Data display is the same as in Fig. 3. (c) Sequence of 1-km WSR-88D 0.5° base reflectivities from Raleigh, NC, at 0001–0232 UTC 8 Mar 2004. Intensity scale (dBZ) given in vertical bar on left side of each frame. Largely uniform, blue-shaded areas centered on radar location (center right) at 0001, 0031, 0101, and 0131 UTC are ground clutter.

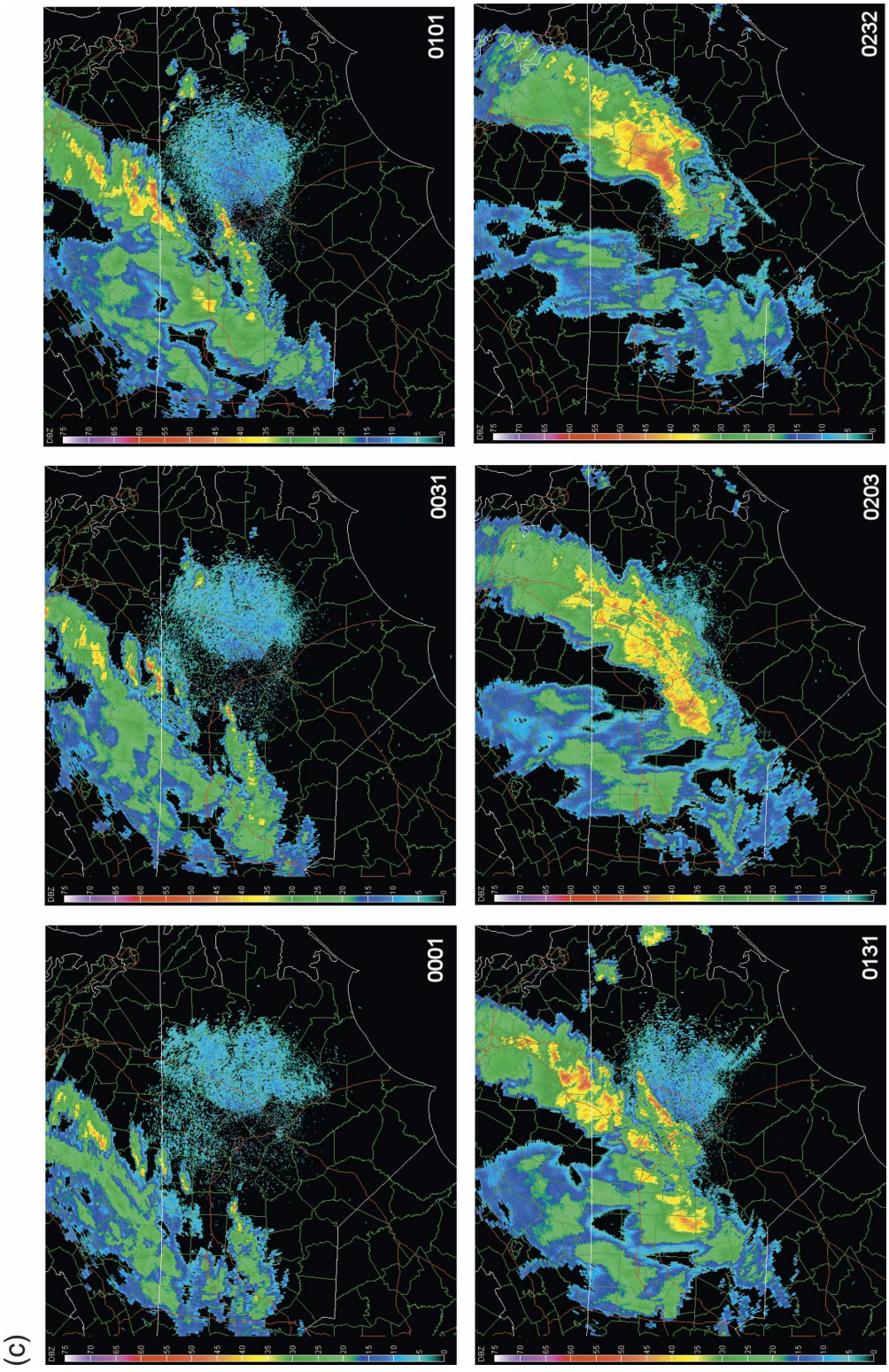

FIG. 10. (*Continued*)

(a)

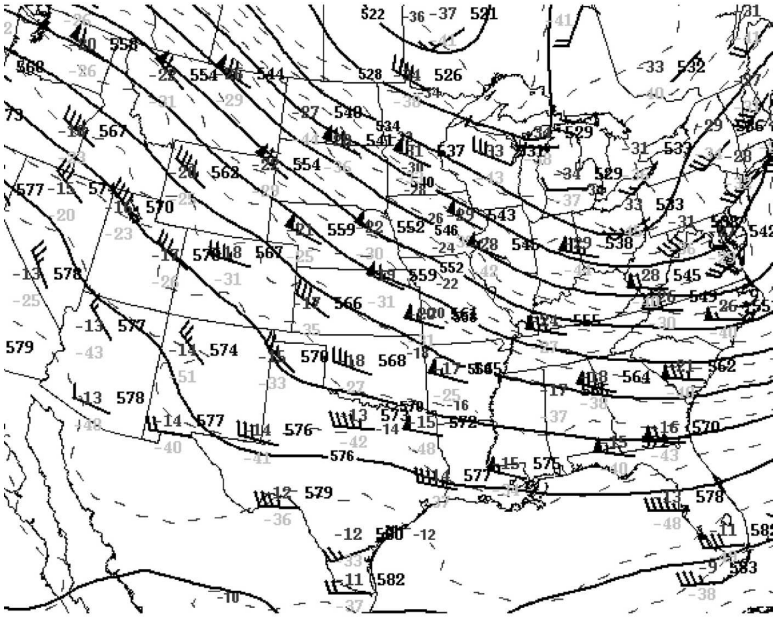

(b)

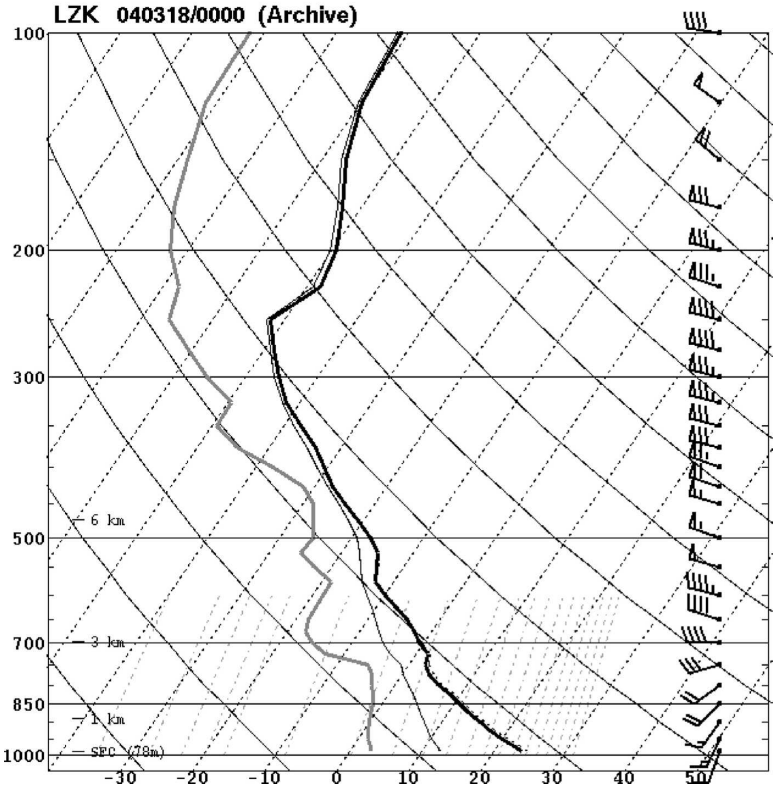

FIG. 11. (a) As in Fig. 10a but at 0000 UTC 18 Mar 2004. (b) As in Fig. 10b but for Little Rock, AR, at 0000 UTC 18 Mar 2004. (c) As in Fig. 10c but from Fort Smith, AR, at 0201–0506 UTC 18 Mar 2004, and with station model format as in Fig. 6. Areas of largely uniform, blue-shaded returns in western and southern sectors of the displays are ground clutter.

(c)

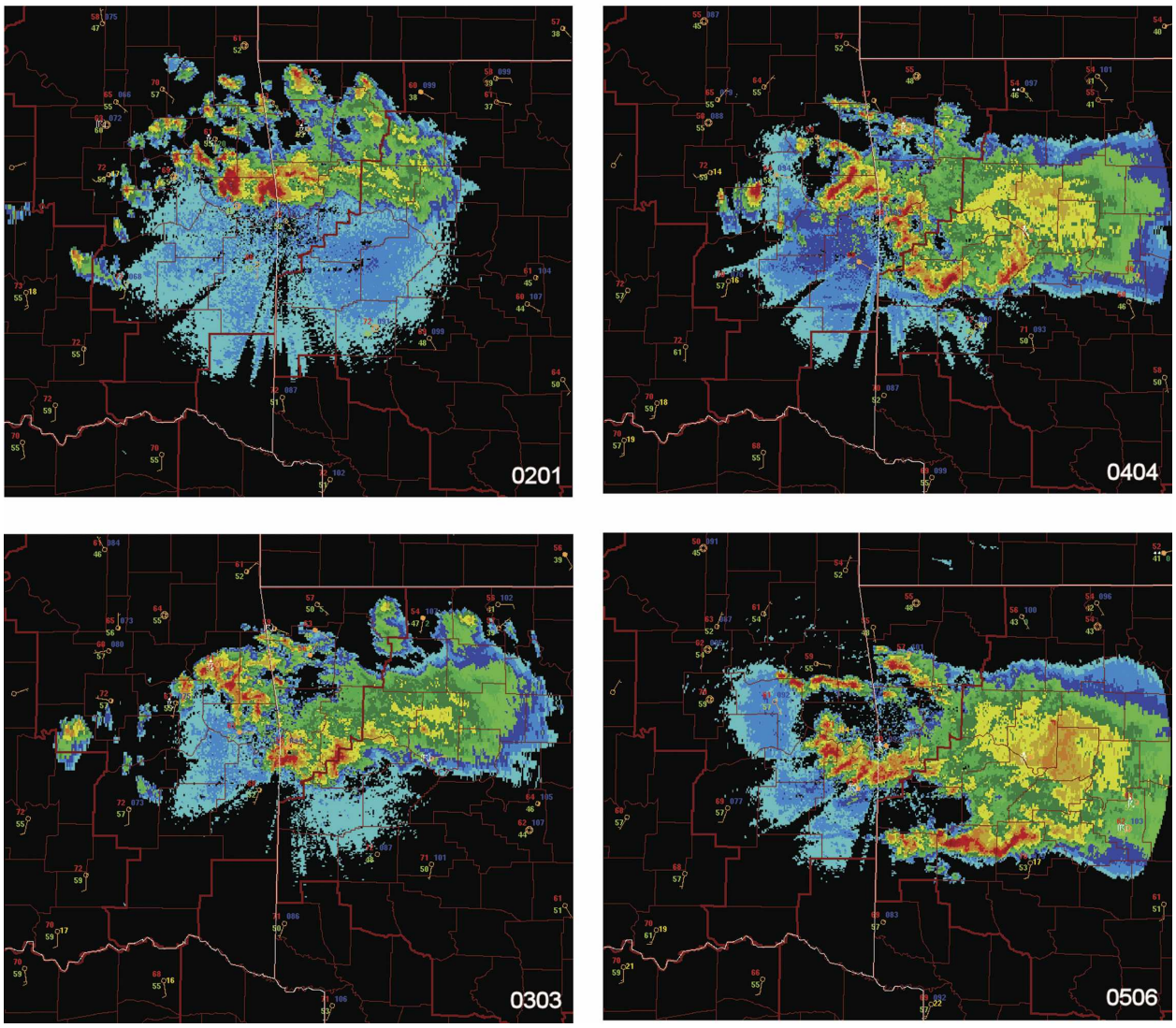

FIG. 11. (*Continued*)

tures and dewpoints were lower (Fig. 11c). As a result, there was a westward component to the cell propagation, and the system exhibited more rightward movement relative to the mean flow than did the two other warm events.

Comparison of Fig. 10c with Fig. 11c shows that average radar reflectivities during the period of high wind production in western Arkansas were somewhat stronger (with a few cells greater than 50 dBZ) than in the North Carolina case. This reflects the fact that some of the incipient convection in Oklahoma included hail-producing supercells, as CAPE in that area was rather substantial (around 1000 J kg^{-1}; not shown) during the afternoon. But the storms had weakened by the time wind damage began to occur and the convection assumed LDD characteristics over Arkansas around 0215 UTC.

To examine the origin of the steep lower-tropospheric lapse rates present in both events just discussed, back parcel trajectories for the LDD initiation locations near the time of system genesis are presented in Fig. 12. The trajectories were computed for parcels at the 1000, 1500, and 3000 m AGL levels using the National Oceanic and Atmospheric Administration/Air Resources Laboratory's (NOAA/ARL) Hybrid Single-Particle Lagrangian Integrated Trajectory HYSPLIT) model, which was developed for computing air parcel trajectories in dispersion and deposition studies

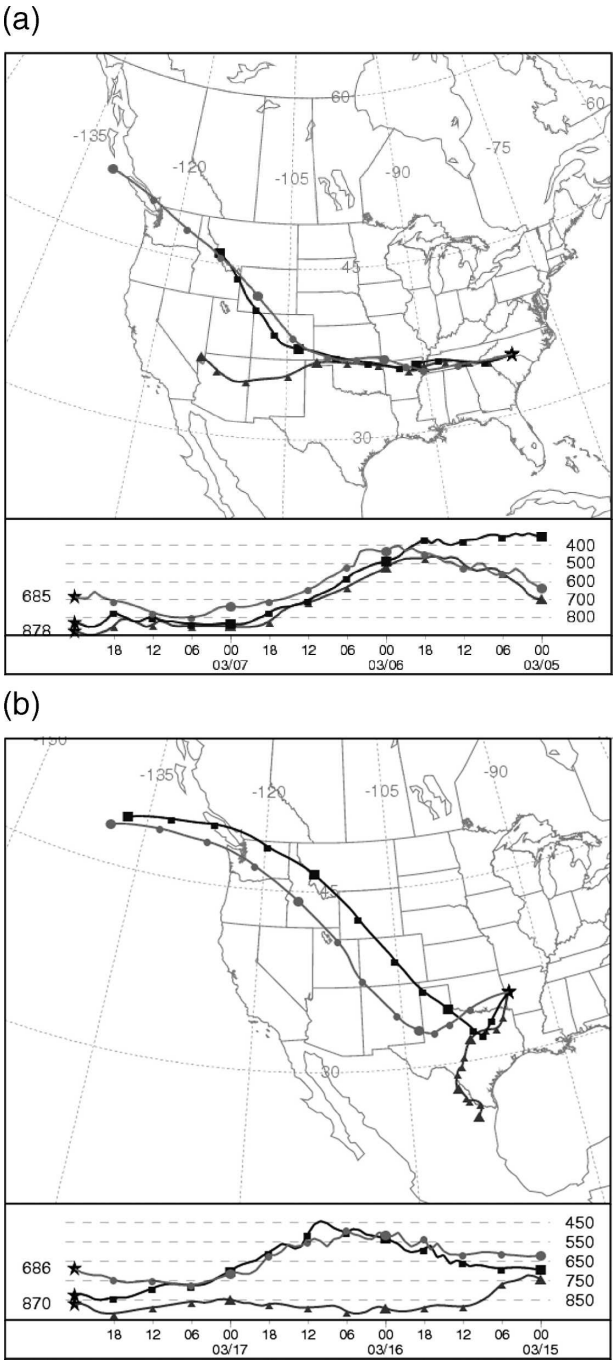

FIG. 12. (a) NOAA/ARL HYSPLIT model back trajectories of the 1000 m (dark gray lines with triangles), 1500 m (black lines with squares), and 3000 m (medium gray lines with circles) AGL parcels ending at 0000 UTC 8 Mar 2004 for the LDD initiation location indicated by the black star. Bottom panel depicts parcel height (mb; scale on the right) at the indicated month, date, and hour (UTC). Larger circles, squares, and triangles used at 24-h intervals. (b) Same as (a) but for the LDD initiation location indicated by the black star at 0000 UTC 18 Mar 2004.

(Draxler and Rolpf 2005). As it may be accessed online (information available at http://www.arl.noaa.gov/ready/hysplit4.html), it provides a convenient way to track air parcel motion for use in severe weather case studies.

As Fig. 12 shows, boundary layer parcels in both events originated over the elevated terrain of the western United States. The three parcels sampled show a recent (24–48 h) history of descent in the 8 March cool event. This suggests that differential subsidence on the anticyclonic side of the associated midlevel jet streak (not shown) may have been a contributing factor in enhancing the steep lower-tropospheric lapse rates observed with this strongly forced event. Meanwhile, the 1000-m parcel exhibits minimal height change during the 48 h prior to the 18 March warm event, implying that the steep boundary layer lapse rates in this case were related more to recent surface heating than to dynamic effects.

5. Concluding remarks

This study has presented data on a subset of forward-propagating, damaging wind-producing convective systems that we have termed low-dewpoint derechos. These systems occur in relatively dry lower-tropospheric environments characterized by very limited CAPE.

Because the LDD environment is not conducive to deep, moist convective development, a source of strong mesoscale forcing for ascent (such as a well-defined cold front or wind shift line) is necessary to initiate the first storms that subsequently "jump start" LDD formation. Once developed, we hypothesize that LDDs are then maintained by a thermodynamic and kinematic environment that supports organized, downwind cell propagation along storm outflow. Deeply mixed boundary layers, in conjunction with moderate to strong and largely unidirectional mean flow above the boundary layer, appear to promote an organized microburst convective mode in which the incipient MCSs are sustained by a series of downwind-directed microbursts. The microbursts foster discrete downstream propagation of the convective systems until the potential for convective initiation and subsequent cold downdraft production ultimately diminishes.

Given the propensity for microbursts to occur during afternoon or early evening (e.g., Wakimoto 1985), it is not surprising that a similar diurnal peak in LDD occurrence appears in the present dataset (Table 1). Note, however, that several LDDs developed in mid- to late morning, and that two initiated after sunset. These observations reflect the conditionally unstable environment associated with LDD genesis and illustrate that

strong forcing for ascent is likely a necessary ingredient for achieving convective initiation in LDDs.

As previously noted, the LDDs in this study occurred in the exit region of mid- to upper-level jet streaks. The events were, however, associated with a wide range of large-scale jet orientations. Coupled with the data presented regarding the mean thermodynamic environment conducive to LDD genesis, it seems reasonable to conclude that the jet orientation most favorable for LDDs likely varies both seasonally and geographically across the country. The limited number of cases examined, however, necessarily precludes a definitive statement on this topic. Similarly, at best we can only speculate as to the true geographical distribution of LDDs. But the mean analyses do provide clues as to why the systems thus far have not been observed over either the Gulf Coast region or the far western United States. Considering that the primary source region of steep low- to midlevel lapse rates is the Colorado and Mexican Plateaus and Rockies, and that sustained cyclonic upper-level flow regimes favor the northern states, it would appear that both the far West and the Gulf Coast are climatologically situated somewhat unfavorably for LDD development. Similarly, the mean thermodynamic fields suggest that LDDs are probably least likely to develop during late summer and early fall. Indeed, no LDDs are known to have occurred during this period in recent years.

While this paper has described some characteristics of the synoptic- and meso-alpha-scale LDD environment, considerably more information is needed on the storm scale before the location and intensity of the hazardous winds that LDDs produce can be forecast reliably. For example, while it appears that dry air and steep lapse rates are conducive to LDD development and maintenance, subtle changes in the distribution and temporal evolution of these factors probably account for some of the "null" LDD events occasionally observed. Further, given the apparent importance of convectively induced downdrafts on LDD development, complex cloud microphysical processes must be quantified before accurate forecasts become a reality. A disproportionate number of the events studied here occurred during the cool season. Does this simply reflect the fact that atmospheric moisture content is lower at that time of the year, or perhaps that melting and/or sublimation processes are important to LDD development? Just prior to the submission of this manuscript, an LDD that occurred in Iowa and Illinois on 12 February 2003 came to the attention of the authors. Synoptically, the system appears to closely fit the LDD pattern described in section 3, with the exception that the environmental profile was so cold that snow rather than rain occurred at the surface. While this case suggests that the presence of melting is not a necessary condition for LDD development, it does not preclude the possibility that considerable sublimation may have occurred. Clearly, additional studies, preferably those that blend both observational and modeling techniques, are needed to better understand LDDs.

Acknowledgments. The authors thank David Bright for the creation of the GEMPAK backgrounds used in Fig. 2, and for his many comments and suggestions. We also thank Mike Coniglio, Dave Schultz, Steve Weiss, and an anonymous reviewer very much for insightful comments that improved the manuscript. John Hart and Jason Levit provided software assistance, and Jared Guyer obtained radar and satellite data for several cases.

REFERENCES

Bentley, M. L., and T. L. Mote, 2000: A synoptic climatology of cool-season derecho events. *Phys. Geogr.,* **21,** 21–37.

Bluestein, H. B., and P. C. Banacos, 2002: The vertical profile of wind and temperature in cyclones and anticyclones over the eastern two-thirds of the United States: A climatology. *Mon. Wea. Rev.,* **130,** 477–506.

Burke, P. C., and D. M. Schultz, 2004: A 4-yr climatology of cold-season bow echoes over the continental United States. *Wea. Forecasting,* **19,** 1061–1074.

Chappell, C. F., 1986: Quasi-stationary convective events. *Mesoscale Meteorology and Forecasting,* P. S. Ray, Ed., Amer. Meteor. Soc., 289–310.

Coniglio, M. C., D. J. Stensrud, and M. B. Richman, 2004: An observational study of derecho-producing convective systems. *Wea. Forecasting,* **19,** 320–337.

Corfidi, S. F., 2003: Cold pools and MCS propagation: Forecasting the motion of downwind-developing MCSs. *Wea. Forecasting,* **18,** 997–1017.

Doswell, C. A., III, H. E. Brooks, and M. P. Kay, 2005: Climatological estimates of daily local nontornadic severe thunderstorm probability for the United States. *Wea. Forecasting,* **20,** 577–595.

Draxler, R. R., and G. D. Rolpf, cited 2005: NOAA/ARL HYSPLIT model. [Available online at http://www.arl.noaa.gov/ready/hysplit4.html.]

Evans, J. S., and C. A. Doswell III, 2001: Examination of derecho environments using proximity soundings. *Wea. Forecasting,* **16,** 329–342.

Fenelon, E. C., 1998: Doppler radar analysis of a microburst producing bow echo associated with a high shear and very low CAPE environment. Preprints, *19th Conf. on Severe Local Storms,* Minneapolis, MN, Amer. Meteor. Soc., 490–494.

Johns, R. H., 1993: Meteorological conditions associated with bow echo development in convective storms. *Wea. Forecasting,* **8,** 294–299.

——, and W. D. Hirt, 1987: Derechos: Widespread convectively induced windstorms. *Wea. Forecasting,* **2,** 32–49.

——, K. W. Howard, and R. A. Maddox, 1990: Conditions associated with long-lived derechos—An examination of the large-scale environment. Preprints, *16th Conf. on Severe Local Storms,* Kananaskis Park, AB, Canada, Amer. Meteor. Soc., 408–412.

Orlanski, I., 1975: A rational subdivision of scales for atmospheric processes. *Bull. Amer. Meteor. Soc.,* **56,** 527–530.

Przybylinski, R. W., 1995: The bow echo: Observations, numerical simulations, and severe weather detection methods. *Wea. Forecasting,* **10,** 203–218.

Schaefer, J. T., and C. A. Doswell III, 1979: On the interpolation of a vector field. *Mon. Wea. Rev.,* **107,** 458–476.

Schultz, D. M., 2005: A review of cold fronts with prefrontal troughs and wind shifts. *Mon. Wea. Rev.,* **133,** 2449–2472.

van den Broeke, M. S., D. M. Schultz, R. H. Johns, J. S. Evans, and J. E. Hales, 2005: Cloud-to-ground lightning production in strongly forced, low-instability convective lines associated with damaging wind. *Wea. Forecasting,* **20,** 517–530.

Wakimoto, R. M., 1985: Forecasting dry microburst activity over the high plains. *Mon. Wea. Rev.,* **113,** 1131–1143.

——, 2001: Convectively driven high wind events. *Severe Convective Storms, Meteor. Monogr*., No. 50, Amer. Meteor. Soc., 255–298.

Weiss, S. J., J. A. Hart, and P. R. Janish, 2002: An examination of severe thunderstorm wind report climatology: 1970–1999. Preprints, *21st Conf. on Severe Local Storms,* San Antonio, TX, Amer. Meteor. Soc., 446–449.

Wolf, R., 1998: Evolution and structure of a low-topped severe squall line. Preprints, *19th Conf. on Severe Local Storms,* Minneapolis, MN, Amer. Meteor. Soc., 480–483.